

Supplementary material for:

Facile multifunctional plasmonic sunlight harvesting with tapered triangle nanopatterning of thin films

Giulia Tagliabue¹, Hadi Eghlidi^{1,*}, Dimos Poulikakos^{1,*}

¹ Laboratory of Thermodynamics in Emerging Technologies, Institute of Energy Technology, Department of Mechanical and Process Engineering, ETH Zürich, CH-8092 Zürich, Switzerland

* email: (H.E.) hadi.eghlidi@lntn.iet.mavt.ethz.ch; (D.P.) dpoulikakos@ethz.ch

S1. Description of the geometry

As illustrated in Figure S1b, the angle θ is half of the opening angle of the tips of the triangles. Employing the definition of similar triangles in Euclidian geometry, we define similar concave triangles having the same tip opening angle, 2θ . It can be easily observed that keeping the ratio $\Delta R/R_{\text{bead}}$ constant leads to a constant θ and therefore, similar curved triangles. On the other hand, decreasing ΔR for a given R_{bead} , leads to smaller θ values and therefore, sharper tips. Decreasing ΔR also yields smaller d values (closer tips). In the simulations reported in Figures 2b,c the triangles are kept similar while R_{bead} is varied.

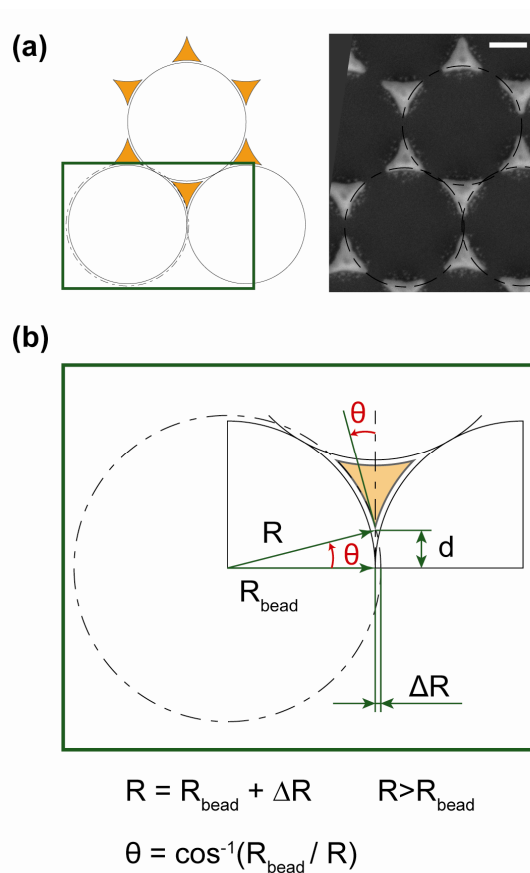


Fig. S1 | Definition of the geometrical parameters. (a) Top view of a unit cell of the gold front pattern. Left: schematics Right: experimental realization. Scale bar is equal to 100 nm. (b) Magnified schematics of the highlighted area in part (a) with definition and equations for the main geometrical parameters.

S2. Dip-coating Set-up

The dip-coating set-up is placed inside a closed plexiglass chamber which is equipped with humidity and temperature sensors. The humidity can be actively controlled and set to a desired value: a flow of dry nitrogen is passed through a glass bottle containing an ultrasonic vaporizer which can produce variable amounts of fine water fog.

The core of the dip-coating set-up is the linear micro stage (M-112.1DG, PI-Physik Instrumente) controlled by a DC servo motor (C-863.11, PI-Physik Instrumente). These two components ensure a smooth movement even at very low speeds, preventing disturbances of the meniscus motion due to uneven displacements.

The sample is dipped into a home-made glass well (WxDxH \approx 30x6x20mm).

S3. Main works Overview

Absorber	Range (Bandwidth)	Absorption (average)	Angle Insensitive	Polarization Insensitive	Overall Thickness	Fabrication method	Scalability ^{ref}
Crossed trapezoidal arrays – Aydin et al. ¹⁴	400-700nm (300nm)	>50%* (71%)	Yes (0°-70°)	Yes	260 nm	E-beam lithography (top structure)	Poor; good if coupled with nano-imprint techniques ¹
Ultra-sharp convex grooves – Sondergaard et al. ¹⁹	450-850nm (400nm)	>87% (96%)	Not Measured	Yes (if re-deposition of gold is limited)	900 nm	FIB milling	Very poor ²
Circularly-shaped gap plasmon resonators – Nielsen et al. ¹⁵	400-850nm (450nm)	>80%* (89%)	Yes (0°-40°)	Yes (very little sensitivity)	170 nm	E-beam lithography (top structure)	Poor; good if coupled with nano-imprint techniques ¹
Nanocomposite materials – Hedayati et al. ¹⁷	400-750nm (350nm)	>87%* (-)	Yes (0°-60°)	Yes (very little sensitivity)	145 nm	Sputtering	Very good
Tapered triangle nanopattern – Tagliabue et al.	380-980nm (600nm)	>67% (88%)	Yes (0°-45°)	Yes	260 nm	NSL (top structure)	Good

(*) value estimated from the paper figures.

Table S1: Overview of main works in the field of plasmonic broadband absorbers. This table compares quantitatively the performances of some important designs of plasmonic broadband absorbers proposed in the literature in recent years. Reference numbers in the first column are according to the main text.

S4. Grating-coupled surface plasmon polariton (SPP)

A three layer system, air-glass-gold, can support surface plasmon polaritons (SPP) with the following dispersion relation:³

$$e^{-4k_1 \frac{h_{\text{SiO}_2}}{2}} = \frac{\frac{k_1}{\varepsilon_1} + \frac{k_2}{\varepsilon_2}}{\frac{k_1}{\varepsilon_1} - \frac{k_2}{\varepsilon_2}} \cdot \frac{\frac{k_1}{\varepsilon_1} + \frac{k_3}{\varepsilon_3}}{\frac{k_1}{\varepsilon_1} - \frac{k_3}{\varepsilon_3}}$$

$$\text{with } k_i^2 = \beta^2 - k_0^2 \varepsilon_i \text{ for } i = 1, 2, 3$$

Materials 1,2,3 are indicated in Figure S2a, β is the SPP wavevector and k_i 's and ε_i 's are the vertical wavevector components and permittivities, respectively. The dispersion curve (ω vs. β) is reported in Figure S2b.

The presence of a grating (in this case the array of tapered triangles) provides coupling of the normally incident light to SPP. The wavevector of the excited SPP is given by $\beta = K_{\text{grating}}$ (see Figure S2a) which corresponds to the frequency $\omega(\beta)$ (see Figure S2b).⁴

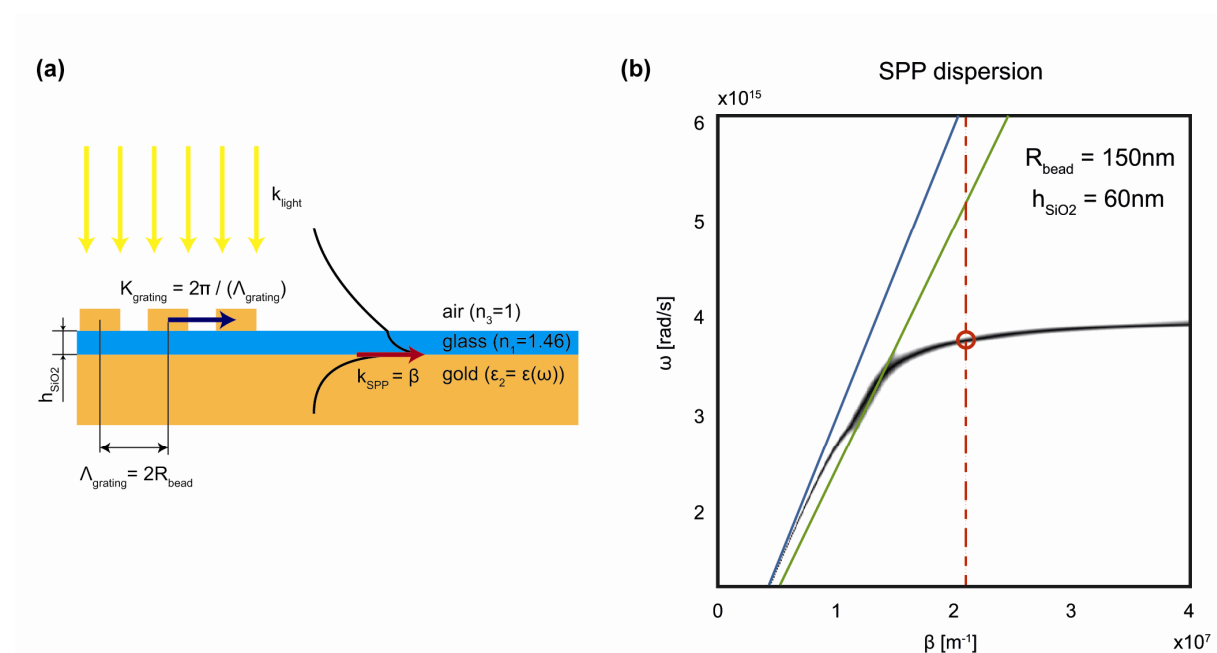


Fig. S2: SPP excitation and dispersion curve. (a) Schematic representation of grating-coupled SPP excitation for the multilayer air-glass-gold system. In the case of normal incidence the condition $\beta = K_{\text{grating}}$ has to be satisfied. (b) Black curve: SPP dispersion curve for the multilayer system illustrated in part (a). Blue line: air light line. Green line: glass light line. Dash-dotted vertical line: $\beta = K_{\text{grating}}$ for the case of $R_{\text{bead}} = 150$ nm. The frequency ω is the intersection of the black curve and the vertical line (red circle, $\omega = 3.779e^{15}$ rad/s corresponding to $\lambda = 498$ nm).

S5. Absorption efficiency of an isolated tapered triangle on glass

We simulated an isolated tapered triangle on a glass substrate and calculated the absorption efficiency as:⁵

$$Q_{abs} = \frac{1}{A_{triangle} \cdot \frac{E_0^2}{2\mu_0 c}} \int_V P_{dissipated}$$

The tapered triangle has the same dimensions as the triangles in an array with $R_{bead} = 150$ nm, $\Delta R = 2$ nm and $h_{AuFP} = 100$ nm, which has been studied in the main text.

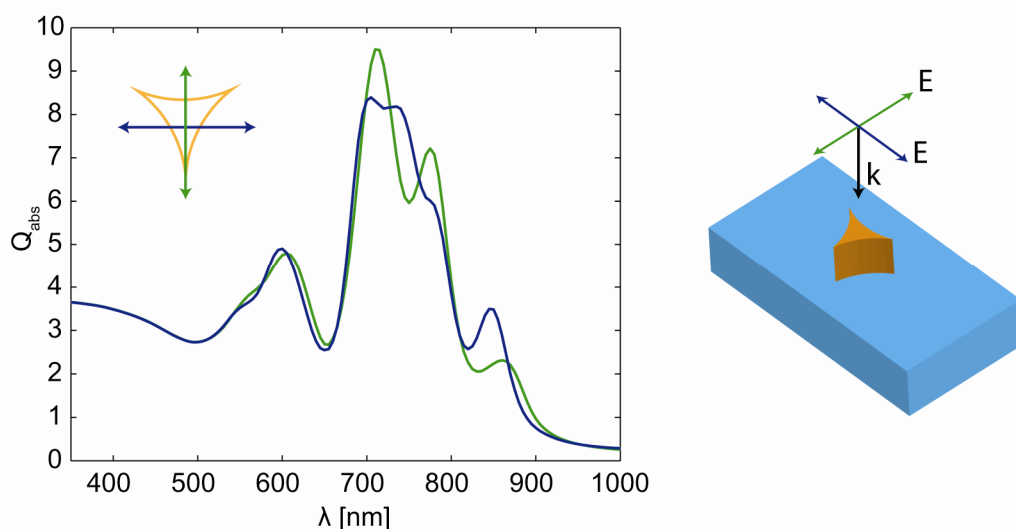


Fig. S3: Absorption efficiency of an isolated tapered triangle. Left: Calculated absorption efficiency, Q_{abs} , for an isolated tapered triangle on glass, excited with two different polarizations. The tapered triangle has the same dimensions as the triangles in an array with $R_{bead} = 150$ nm, $\Delta R = 2$ nm and $h_{AuFP} = 100$ nm. Right: 3D graphical representation of the simulated geometry.

1. Guillot, N.; de la Chapelle, M. L. *J. Nanophotonics* **2012**, *6*, 064501-064506.
2. Escobedo, C. *Lab Chip* **2013**, *13*, (13), 2445-2463.
3. Maier, S. A., *Plasmonics Fundamentals and Applications*. Springer: 2007.
4. Chu, Y. Z.; Crozier, K. B. *Opt Lett* **2009**, *34*, (3), 244-246.
5. Knight, M. W.; Halas, N. J. *New J Phys* **2008**, *10*.